



PAPER

OPEN ACCESS

RECEIVED
11 January 2024REVISED
7 March 2024ACCEPTED FOR PUBLICATION
5 June 2024PUBLISHED
14 June 2024

Original content from
this work may be used
under the terms of the
[Creative Commons
Attribution 4.0 licence](#).

Any further distribution
of this work must
maintain attribution to
the author(s) and the title
of the work, journal
citation and DOI.



Determinants of the dynamic cerebral critical closing pressure response to changes in mean arterial pressure

Ronney B Panerai^{1,2,*} , Abdulaziz Alshehri^{1,3} , Lucy C Beishon^{1,2} , Aaron Davies¹ ,
Victoria J Haunton¹ , Emmanuel Katsogridakis¹ , Man Y Lam¹ , Osian Llwyd^{1,4} ,
Thompson G Robinson^{1,2} and Jatinder S Minhas^{1,2}

¹ Cerebral Haemodynamics in Ageing and Stroke Medicine (CHiASM), Department of Cardiovascular Sciences, University of Leicester, Leicester, United Kingdom

² NIHR Leicester Biomedical Research Centre, BHF Cardiovascular Research Centre, Glenfield Hospital, Leicester, United Kingdom

³ College of Applied Medical Sciences, University of Najran, Najran, Saudi Arabia

⁴ Wolfson Centre for Prevention of Stroke and Dementia, Department of Clinical Neurosciences, University of Oxford, Oxford, United Kingdom

* Author to whom any correspondence should be addressed.

E-mail: rp9@le.ac.uk

Keywords: cerebral blood flow, critical closing pressure, transfer function analysis, cerebral autoregulation, cerebrovascular resistance

Abstract

Objective. Cerebral critical closing pressure (CrCP) represents the value of arterial blood pressure (BP) where cerebral blood flow (CBF) becomes zero. Its dynamic response to a step change in mean BP (MAP) has been shown to reflect CBF autoregulation, but robust methods for its estimation are lacking. We aim to improve the quality of estimates of the CrCP dynamic response. **Approach.** Retrospective analysis of 437 healthy subjects (aged 18–87 years, 218 males) baseline recordings with measurements of cerebral blood velocity in the middle cerebral artery (MCAv, transcranial Doppler), non-invasive arterial BP (Finometer) and end-tidal CO₂ (EtCO₂, capnography). For each cardiac cycle CrCP was estimated from the instantaneous MCAv-BP relationship. Transfer function analysis of the MAP and MCAv (MAP-MCAv) and CrCP (MAP-CrCP) allowed estimation of the corresponding step responses (SR) to changes in MAP, with the output in MCAv (SRV_{MCAv}) representing the autoregulation index (ARI), ranging from 0 to 9. Four main parameters were considered as potential determinants of the SRV_{CrCP} temporal pattern, including the coherence function, MAP spectral power and the reconstruction error for SRV_{MAP}, from the other three separate SRs. **Main results.** The reconstruction error for SRV_{MAP} was the main determinant of SRV_{CrCP} signal quality, by removing the largest number of outliers (Grubbs test) compared to the other three parameters. SRV_{CrCP} showed highly significant ($p < 0.001$) changes with time, but its amplitude or temporal pattern was not influenced by sex or age. The main physiological determinants of SRV_{CrCP} were the ARI and the mean CrCP for the entire 5 min baseline period. The early phase (2–3 s) of SRV_{CrCP} response was influenced by heart rate whereas the late phase (10–14 s) was influenced by diastolic BP. **Significance.** These results should allow better planning and quality of future research and clinical trials of novel metrics of CBF regulation.

Abbreviations

ARI	autoregulation index
BP	arterial blood pressure
CA	cerebral autoregulation
CBF	cerebral blood flow
CHiASM	cerebral haemodynamics in ageing and stroke medicine
COH	coherence
CrCP	critical closing pressure

CrCP ₀	mean CrCP
CKSError	checksum error
CVR	cerebrovascular resistance
DBP	diastolic BP
ECG	electrocardiogram
EtCO ₂	end-tidal carbon dioxide
FFT	fast Fourier transform
FMS	Finapres Medical Systems
FORTTRAN	FORmula TRANslation
GLM	General Linear Model
MAP	mean BP
MAP ₀	mean MAP
MAP _{power}	spectral power of MAP
MCA	middle cerebral artery
MCAv	MCA blood velocity
MCAv ₀	mean value MCAv
NMSE	normalised mean square error
P1	first harmonic of BP for one cardiac cycle
PaCO ₂	partial pressure carbon dioxide
PHYSIDAS	physiological data acquisition system
RAP	resistance-area product
RAP ₀	mean RAP
SBP	systolic BP
SML _{corr}	similarity correlation coefficient
SR	step response
SR _{CrCP}	SR of CrCP
SR _{MAP}	SR of MAP
SR _{MCAv}	SR of MCAv
SR _{RAP}	SR of RAP
TCD	transcranial Doppler ultrasound
TFA	transfer function analysis
V1	first harmonic of MCAv for one cardiac cycle
V _{CrCP}	subcomponent of CrCP
V _{MAP}	subcomponent of MAP
V _{MCAv}	subcomponent of MCAv
V _{RAP}	subcomponent of RAP
VSM	vascular smooth muscle

1. Introduction

TFA of the beat-to-beat mean arterial blood pressure (MAP)—cerebral blood velocity signals, often recorded with transcranial Doppler ultrasound (TCD) in the middle cerebral artery (MCAv), has been the dominant approach in physiological and clinical studies of dynamic CA (Claassen *et al* 2016, Nogueira *et al* 2022). CA controls the diameter of cerebral arterioles and smaller blood vessels, to protect the brain from extreme values of MAP (Claassen *et al* 2021). Different from *static* CA, that is assessed with steady-state values of MAP and MCAv, *dynamic* CA is expressed by the transient response of MCAv to rapid changes in MAP (Aaslid *et al* 1989, Tiecks *et al* 1995). From TFA, the frequency dependence of the gain, phase and coherence functions have been shown to reflect changes in dynamic CA effectiveness, in different physiological conditions, and also in pathological states {Claassen *et al* (2016) #2598; Intharakham *et al* (2019) #2779; Panerai (1998b) #1574}. As part of TFA, the effectiveness of dynamic CA can also be assessed with the estimation of the MCAv step response to MAP changes, using the gain and phase information, in combination with the inverse FFT {Claassen *et al* (2016) #2598; Ma *et al* (2016) #2617; Panerai (1998a) #1574; Panerai *et al* (2016) #2614;}. The MCAv step response has been standardised by Tiecks *et al* to provide a scale of Autoregulation Index (ARI) values, ranging from 0 to 9, where zero represents absence of dynamic CA and 9 is the most efficient response that is usually observed (Tiecks *et al* 1995).

One limitation of standard TFA of the MAP-MCAv relationship though, is the use of mean values of pressure and velocity for each heart beat, without taking into consideration the behaviour of these parameters *within* each cardiac cycle. Continuous recordings of arterial blood pressure (BP) and MCAv show temporal patterns that not only vary within each cardiac cycle, but also from beat-to-beat. Noteworthy, the temporal pattern of MCAv is not entirely due to the corresponding temporal pattern of BP, but also depends on changes in the vascular bed, distal to the point of TCD insonation. Characterisation of the dynamic properties of the vascular bed can be fairly complex (McDonald 1974), but a relatively simple and robust model based on the parameters of CrCP and RAP, has been used successfully in many physiological and

clinical studies (Early *et al* 1974, Czosnyka *et al* 1999, Dawson *et al* 1999, Weyland *et al* 2000, Aaslid *et al* 2003, 2007, Buhre *et al* 2003, Soehle *et al* 2004, Ogoh *et al* 2011, van Veen *et al* 2015, Puppo *et al* 2016, Beishon *et al* 2018, Panerai *et al* 2020). As BP is reduced, the CrCP reflects the pressure value at which CBF reaches zero (Burton 1951, Panerai 2003). When the instantaneous MCAv is plotted as a function of BP, RAP corresponds to the inverse of the linear regression slope but can also be derived by alternative methods (Evans *et al* 1988, Panerai *et al* 2011). The relevance of CrCP is its dependence on the VSM active tension and the transmural pressure of small arteries and capillaries (Burton 1951, Panerai 2003). The sensitivity of CrCP to the active tension of VSM is particularly relevant since these are the actuators of CBF regulation, either responding to changes in MAP (dynamic CA), PaCO₂ (vasomotor reactivity), or oxygen demand (neurovascular coupling) (Claassen *et al* 2021). Moreover, the sensitivity of CrCP to transmural pressure make it a very promising metric for the detection of alterations in intracranial (Weyland *et al* 2000, Brasil *et al* 2023) or intrathoracic (Dawson *et al* 1999) pressures.

TFA of the MAP-RAP relationship, or alternatively, the MAP-CVR (cerebrovascular resistance) relationship, has been reported previously (Edwards *et al* 2002, Panerai *et al* 2006, 2011) but we are not aware of TFA of the MAP-CrCP relationship being reported by other groups. In recent studies, we demonstrated the feasibility of deriving the CrCP step response to changes in MAP by means of TFA or autoregressive-moving average modelling (Panerai *et al* 2020, 2021). These studies have shown that the temporal pattern of the CrCP step response is sensitive to changes in arterial CO₂ (Panerai *et al* 2020), and also influenced by the efficiency of dynamic CA (Panerai *et al* 2021). These initial results are encouraging, but need to be interpreted with caution since the temporal pattern of CrCP is highly variable and conclusions have been drawn from population averages with relatively large sample sizes. A better understanding of the determinants of the temporal patterns of both CrCP and RAP step responses to changes in MAP is clearly needed to allow their use in individual subjects, as a necessary step towards demonstrating their potential in clinical applications. To progress in this direction, we have amalgamated a large number of recordings from healthy individuals and investigated the influence of different factors that could affect the quality of estimates, including the coherence function, transfer function reconstruction error and measures of ensemble membership, also taking into consideration the potential effects of sex and age. As described below, these multiparametric analyses demonstrate the feasibility of improving the quality of CrCP step response estimates, as a condition for exploring its potential in future clinical studies.

2. Methods

2.1. Study participants

Data for this study were extracted from the Cerebral Haemodynamics in Ageing and Stroke Medicine (CHiASM) group database. A total of 11 previous studies contributed with baseline recordings in healthy participants. Most of these studies included physiological manoeuvres, in addition to an initial baseline recording. In the present study though, only the 5 min baseline recording at rest in the supine position was included for analysis. All studies in the database had similar inclusion and exclusion criteria. Healthy participants were 18 years of age or older, without any history or symptoms of cardiovascular, neurological or respiratory disease. Individuals with stable and well controlled comorbidities such as hypertension were also included. All studies contained in the database had UK Research Ethics Committee approval. All participants provided written, informed consent to the study, and the studies were conducted in accordance with the declaration of Helsinki.

2.2. Measurements

In all studies, recordings were performed by researchers trained by senior investigators to attain the same quality standards for measurements using identical protocol for subjects in the supine position at rest, with the head elevated at 30°, with minimal auditory or visual distraction. Participants were asked to avoid heavy exercise, caffeine, alcohol and nicotine for at least 4 h before attending the CHiASM research laboratory. In all studies, cerebral blood velocity was recorded from the left middle cerebral artery (MCAv) with transcranial Doppler ultrasound (TCD, Viasys Companion III; Viasys Healthcare, PA, USA) using 2 MHz probes secured in place with a head-frame. In the majority of cases, MCAv was also recorded from the right hemisphere, but in approximately 35% of participants, a second recording was obtained from the posterior cerebral artery instead. For this reason, only the left MCAv was included in the study. BP was recorded continuously using a Finapres/Finometer device (FMS, Finapres Measurement Systems, Arnhem, Netherlands), attached to the middle finger of the left hand. Systolic and diastolic BP were measured by standard brachial sphygmomanometry (OMRON 705IT) before each 5 min recording. The servo-correcting mechanism of the Finapres/Finometer was switched on and then off prior to measurements. Heart rate was derived from a 3-lead ECG. End-tidal CO₂ (EtCO₂) was measured continuously via nasal prongs (Salter

Labs) with a capnograph (Capnograph Plus). Data were continuously recorded onto a data acquisition system (PHYSIDAS, Department of Medical Physics, University Hospitals of Leicester) using a sampling rate of 500 samples s^{-1} .

2.3. Data analysis

All signals were visually inspected to identify artefacts; noise and narrow spikes (<0.1 s) were removed by linear interpolation. All signals were low-pass filtered with an 8th order Butterworth filter with cut-off frequency of 20 Hz, after a median filter had been applied to the MCAv. BP was calibrated at the start of each recording using systolic and diastolic values obtained with sphygmomanometry, using our data editing software written in FORTRAN. The R–R interval was automatically marked from the ECG and following visual inspection, occasional missed marks were manually corrected. CrCP and RAP can be obtained by linear regression of the instantaneous MCAv–BP relationship (Lopez-Magana *et al* 2009) but more robust results are usually obtained using the 1st harmonic method (Panerai *et al* 2011). For each cardiac cycle, the 1st harmonic of the MCAv (V1) and BP (P1) signals were calculated and RAP was given by the ratio V1/P1. From this, CrCP was then calculated for the same cardiac cycle as $CrCP = BP_0 - RAP.MCAv_0$ where BP_0 and $MCAv_0$ are the mean values of BP and MCAv for the same cardiac cycle. The end of each expiratory phase was detected in the EtCO₂ signal, linearly interpolated, and resampled with each cardiac cycle. Mean MAP, systolic (SBP) and diastolic BP (DBP) and MCAv values were calculated for each cardiac cycle. Beat-to-beat data were spline interpolated and resampled at 5 samples s^{-1} to produce signals with a uniform time-base.

A linear model of the instantaneous BP–MCAv relationship can be expressed as $MCAv = (MAP - CrCP)/RAP$ for each cardiac cycle (Panerai 2003). For small changes in RAP, it is possible to express this relationship as (Panerai *et al* 2005, 2020):

$$\Delta MCAv = \Delta MAP - \Delta CrCP - \Delta RAP \quad (1)$$

where Δ represents the absolute change in each of the parameters from the baseline values given by $MCAv_0$, MAP_0 , $CrCP_0$ and RAP_0 . Normalising both sides by $MCAv_0$, leads to:

$$V_{MCA} = V_{MAP} + V_{CrCP} + V_{RAP}. \quad (2)$$

With

$$V_{MAP} = \frac{\Delta MAP}{RAP_0} \quad (3)$$

$$V_{CrCP} = -\frac{\Delta CrCP}{RAP_0} \quad (4)$$

$$V_{RAP} = -\frac{\Delta RAP.MCAv_0}{RAP_0} \quad (5)$$

where V_{MCA} is the fractional change in MCAv during spontaneous fluctuations in MAP, that could also be expressed as a percent change. V_{MAP} , V_{CrCP} and V_{RAP} have been termed the *sub-components* of V_{MCA} (Panerai *et al* 2005), expressing their individual percent contribution to explain the overall changes in V_{MCA} (Panerai *et al* 2005, 2020). Important to note, the negative sign in equations (4) and (5) imply that reductions in CrCP or RAP lead to positive contributions to V_{MCAv} .

TFA of the $V_{MAP} - V_{MCAv}$ relationship was performed using Welch's method (1967) with data segmented with 102.4 s duration and 50% superposition (Claassen *et al* 2016). Mean values of V_{MAP} and V_{MCAv} were removed from each segment and a cosine window was applied to minimise spectral leakage. The squared coherence function, gain and phase frequency responses were calculated from the smoothed auto- and cross-spectra using standard procedures (Panerai *et al* 1998a, Claassen *et al* 2016). The V_{MCAv} step response to the V_{MAP} input was estimated using the inverse FFT of gain and phase (Bendat and Piersol 1986, Panerai *et al* 1998b). ARI was extracted by using the normalised minimum square error (NMSE) fit between the MCAv step response and one of the 10 model ARI curves proposed by Tiecks *et al* (1995). ARI values were only accepted if the mean squared coherence function for the 0.15–0.25 Hz frequency interval was above its 95% confidence limit, adjusted for the corresponding degrees of freedom, and the NMSE was ≤ 0.30 (Panerai *et al* 2016). Similar to the $V_{MAP} - V_{MCAv}$ dynamic relationship, TFA was also performed for the $V_{MAP} - V_{RAP}$ and $V_{MAP} - V_{CrCP}$ relationships, and corresponding step responses were obtained with the inverse FFT (Panerai *et al* 2020).

Based on the linear properties of the FFT, a similar relationship between the responses to a step change in MAP can be written as the summation in equation (2) (Panerai *et al* 2020). By changing the order of the terms in equation (2), it is possible to express the step response change in MAP as:

$$SRV_{MAP}^* = SRV_{MCAv} - SRV_{CrCP} - SRV_{RAP} \quad (6)$$

where SRV_{MAP}^* is an estimate of the MAP step response change, based on the summation of the three other step responses (SR). Therefore, the expression above works as a 'checksum' for the accuracy of the three distinct SR estimated for V_{MCAv} , V_{CrCP} and V_{RAP} . As described below, the closer SRV_{MAP}^* is to a perfect step of MAP, the better the quality of estimates will be, thus increasing our confidence in these estimates.

2.4. Statistical analysis

SRV_{MCAv} was only accepted based on the dual criteria of coherence above the 95% confidence limit and a $NMSE \leq 0.30$ for fitting of the Tiecks model (Tiecks *et al* 1995, Panerai *et al* 2016). For statistical analyses, the temporal pattern of each SR was described by the mean values of SR in three distinct time intervals: $T1$ (-0.6 – 1.2 s), $T2$ (2 – 3 s) and $T3$ (10 – 14 s). $T1$ corresponds to the peak of the SRV_{MCAv} , $T2$ the beginning of the V_{MCAv} recovery after the MAP step change, and $T3$ to the tail of the responses (figures 2 and 3). SRV_{CrCP} values for each of these time intervals are represented by SRV_{CrCP}^{Tj} , where $j = 1, 2, \text{ or } 3$, respectively.

Determinants of the SRV_{CrCP} temporal pattern were assessed based on parameters that could influence the quality of estimates. These were (i) the coherence for the $V_{MAP} - V_{CrCP}$ transfer function (COH_{CrCP}), (ii) the mean MAP spectral power in the frequency range (MAP_{power}), (iii) the correlation similarity (SML_{corr}) and (iv) the checksum error (CKS_{error}). COH_{CrCP} was calculated as the mean coherence in the frequency interval 0.02 – 0.30 Hz (Panerai *et al* 2018). MAP_{power} was obtained from the auto-spectrum of MAP, as part of any of the three TFAs. SML_{corr} was the mean correlation coefficient of each SRV_{CrCP} response with all the other corresponding responses. CKS_{error} was the mean square reconstruction error for SRV_{MAP} , obtained from equation (6), in comparison with the original MAP step function, normalised in percent of the step amplitude. A hierarchical sensitivity analysis was performed to assess the influence of the potential determinants on the SRV_{CrCP} temporal pattern and precision of its values at $T1$, $T2$ and $T3$. For each of the four determinants, statistical criteria were adopted to reject values using a simple threshold in each case. For COH_{CrCP} , the threshold was the 95% confidence limit of $COH_{CrCP} > 0.17$, previously established in a bootstrap study (Panerai *et al* 2018). For MAP_{power} , the threshold was determined by the lower 5% confidence limit for the distribution of all values in the current sample. Similar approach was adopted to determine the upper 95% confidence limit for CKS_{error} . Finally, for SML_{corr} , a bootstrap simulation was performed to determine the 95% confidence limit for the null hypothesis, for the mean correlation coefficient between each SRV_{CrCP} estimate and all the other subjects in the study. The number of samples used for each correlation coefficient was $n = 100$, corresponding to a SRV_{CrCP} duration of 20 s. The hierarchical sensitivity analysis was performed separately for each SRV_{CrCP}^{Tj} , $j = 1, 2, \text{ or } 3$, by using Grubbs' test statistic for outliers (1950). The parameter whose threshold removed data leading to the largest reduction in Grubbs' statistic was chosen to top the ranking and the same procedure was repeated with recurrent application to the other three parameters.

To assess the influence of potential physiological determinants of the SRV_{CrCP} response, a number of variables were considered, namely: age, sex, ARI, and the mean values MAP_0 , $MCAv_0$, SBP_0 , DBP_0 , heart rate, $CrCP_0$, RAP_0 and $EtCO_2$ for the 5 min duration of the baseline recording. GLM was employed to assess the significance of these potential determinants and multiple linear regression was used to quantify the strength of their effects on SRV_{CrCP}^{Tj} . Because of the large sample size, normality was assumed for all parameters and variables, confirmed by Q-plots. Statistical analyses were performed with version 7 of *STATISTICA*®. A p -value of <0.05 indicated statistical significance.

3. Results

A total of 459 recordings from healthy subjects were extracted from the CHiASM database. Of these, 22 recordings did not meet the statistical criteria for acceptance of the SRV_{MCAv} step response (Panerai *et al* 2016), resulting in a total of 437 subjects (218 males) who were included in the subsequent analyses. The age of participants ranged from 18–87 years old, without a significant difference between males and females (table 1). Females had a higher $MCAv$ and heart rate, but lower SBP , $EtCO_2$ and RAP when compared to males (table 1).

3.1. Determinants of the SRV_{CrCP} quality

The distributions of CKS_{error} and MAP_{power} for the 437 subjects with accepted SRV_{MCAv} , led to 95% upper and 5% lower confidence limits of 10% and 0.06 mmHg^2 , respectively, which were used as thresholds in the

Table 1. Demographic and physiological characteristics of 437 healthy subjects stratified by sex.

Variable	All subjects ($n = 437$)	Male ($n = 218$)	Female ($n = 219$)	p -value
Age (years)	47.5 ± 17.9	48.5 ± 17.8	46.4 ± 17.9	0.24
MAP (mmHg)	89.7 ± 12.9	90.1 ± 12.6	89.0 ± 13.5	0.45
SBP (mmHg)	130.0 ± 21.1	133.1 ± 20.8	127.0 ± 21.0	0.0023
DBP (mmHg)	70.9 ± 11.9	71.0 ± 12.1	70.8 ± 11.7	0.54
MCAv (cm.s ⁻¹ .mmHg ⁻¹)	55.4 ± 14.7	50.4 ± 13.1	60.9 ± 14.4	<0.0001
EtCO ₂ (mmHg)	39.2 ± 3.9	39.8 ± 4.3	38.5 ± 3.4	0.001
Heart rate (bpm)	65.9 ± 9.8	62.2 ± 9.8	67.9 ± 9.2	0.0006
CrCP (mmHg)	29.3 ± 15.2	28.8 ± 14.2	29.8 ± 16.1	0.51
RAP (mmHg.s.cm ⁻¹)	1.26 ± 0.69	1.40 ± 0.77	1.13 ± 0.57	<0.0001

Values are mean ± SD. MAP: mean arterial blood pressure; SBP: systolic blood pressure; DBP: diastolic blood pressure; MCAv: middle cerebral artery blood velocity; EtCO₂: end-tidal CO₂; CrCP: critical closing pressure; RAP: resistance-area product. P -values for the difference between males and females with Student's t -test.

Table 2. Reduction in Grubbs test statistic for outliers, with cumulative application of four distinct statistical criteria.

	Original dataset	CKS _{error} < 10%	SML _{corr} > 0.008	COH _{CrCP} > 0.17	MAP _{power} > 0.06
n	437	416	344	283	269
SRV ^{T1} _{CrCP}	15.91 [#]	5.44 [#]	5.45 ^{\$}	5.55 ^{\$}	5.79 ^{\$}
SRV ^{T2} _{CrCP}	14.34 [#]	4.60 [#]	4.43 [#]	4.00 [#]	4.08 [#]
SRV ^{T3} _{CrCP}	11.60 [#]	3.93 ^{\$}	4.28 [#]	3.55	3.23

n : sample size after cumulative application of each statistical criterion, SRV^{Tj}_{CrCP}: Step response for the critical closing pressure sub-component (V_{CrCP}) at times $T1$, $T2$ and $T3$; CKS_{error}: checksum error for the reconstructed SR_{MAP}, SML_{corr}: similarity correlation; COH_{CrCP}: coherence for the $V_{MAP} - V_{CrCP}$ transfer function; MAP_{power}: mean spectral power of MAP. [#] $p < 0.01$, ^{\$} $p < 0.05$.

hierarchical sensitivity analysis. Based on the total sample number, the 95% confidence limit for SML_{corr} was 0.008 (figure 1). The bootstrap simulation, to obtain the 95% confidence limit of SML_{corr}, showed a sharp reduction as a function of the number of correlation coefficients averaged (figure 1). To facilitate calculation of this threshold in future studies, a third-order polynomial interpolation resulted in $SML^{95\%} = 0.162 - 0.163z + 0.0622z^2 - 0.0085z^3$, where $z = \log_{10}(N_{averages})$, figure 1). Grubb's test for outliers showed that CKS_{error} > 10% was the main determinant of outliers for SRV^{Tj}_{CrCP} for the three time intervals ($j = 1, 2, 3$), with the loss of 21 samples above the 10% threshold (table 2). In second place, came SML_{corr} > 0.008, with a much smaller reduction in Grubbs' statistic and the loss of an additional 72 subjects from the sample (table 2). The criterion based on COH_{CrCP} > 0.17 was third in the ranking and together with BP_{power} > 0.06 mmHg², had very minor contribution to reduce Grubbs' statistic (table 2). Given the results in table 2, the remainder of the analysis was based on the 416 subjects who met the CKS_{error} < 10% criterion, given the very minor contribution from the other three criteria to reduce Grubbs' statistic further. Figure 2 illustrates the reduction in the scatter of SRV^{Tj}_{CrCP} ($j = 1, 2, 3$) values who met the CKS_{error} < 10% criterion. Representative recordings from one subject who met this criterion, and another who did not, are given in figure 3. Both subjects are above 60 years of age and have similar ARI values but very different values of CKS_{error} that led to the rejection of the SRV_{CrCP} response in figure 3(F). Noteworthy, the corresponding temporal pattern of SRV_{MAP} (figure 3(H)) confirms the poor reconstruction expressed by CKS_{error} = 18%.

3.2. Physiological determinants of SRV_{CrCP}

GLM analysis of repeated measures of $T1 - T3$, with sex as a categorical variable and age and the other potential physiological determinants as continuous co-variates (see Methods), confirmed highly significant differences in the temporal pattern of SRV_{CrCP} due to time ($p < 0.001$), but ruled out any effects of sex ($p = 0.60$) or age ($p = 0.70$). The physiological determinants that showed significant effects were further considered in multiple linear regression modelling, with the ARI and CrCP₀ showing significant

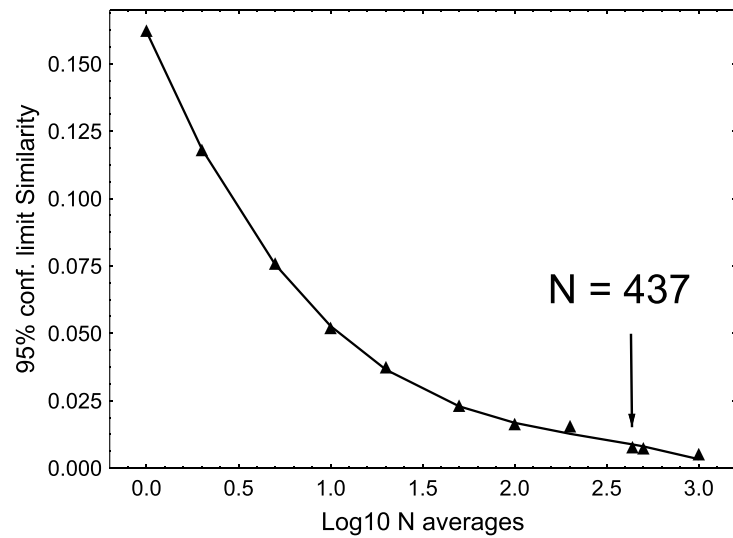


Figure 1. 95% confidence limit for the Similarity Correlation coefficient (SML_{corr}) as a function of the number of correlation values averaged for each subject in log10 scale. The vertical arrow marks the sample number of the present study. Triangles correspond to the confidence limits estimated with bootstrap simulation of the null hypothesis. The continuous line is a third order polynomial interpolation (coefficient values given in the main text).

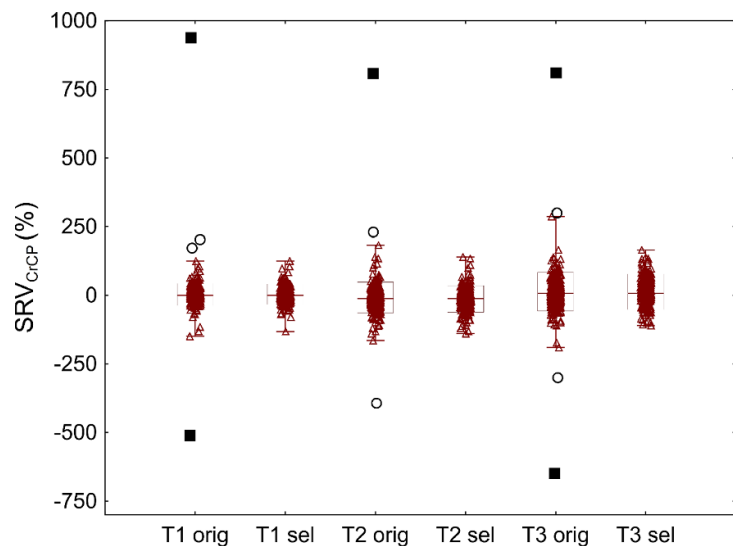


Figure 2. Original (orig) and selected (sel) values of SRV_{CrCP} at time intervals T1–T3 (see Methods). Original values from 437 subjects showing the extreme values (squares), outliers (circles), 5%–95% percentiles (boxes) and median values (horizontal bar) and non-outlier range (whiskers). Open triangles are raw data values. Selected values correspond to data from 416 subjects who met the criterion $CKS_{error} < 10.0\%$.

contributions to explain the variability of SRV_{CrCP}^{Tj} ($j = 1, 2, 3$) (table 3). Heart rate was an additional independent determinant of SRV_{CrCP}^{T2} and DBP_0 also contributed to SRV_{CrCP}^{T3} (table 3).

Stratifying the population averages by three ranges of ARI, led to markedly different temporal patterns for SRV_{CrCP} and, as expected, for SRV_{MCAv} and SRV_{RAP} as well (figure 4).

4. Discussion

4.1. Main findings

Based on a large sample of recordings from healthy participants, we have identified an objective approach that can be used to reduce the variability of SRV_{CrCP} estimates and provide more physiologically plausible temporal patterns. The application of the $CKS_{error} < 10\%$ criterion in future physiological and clinical studies will bring benefits in their quality and reliability. The confirmation that the efficiency of dynamic CA, as expressed by the ARI metric, has a strong influence on the temporal pattern of SRV_{CrCP} should also encourage future studies. The main aim would be to explore the potential additional information that could

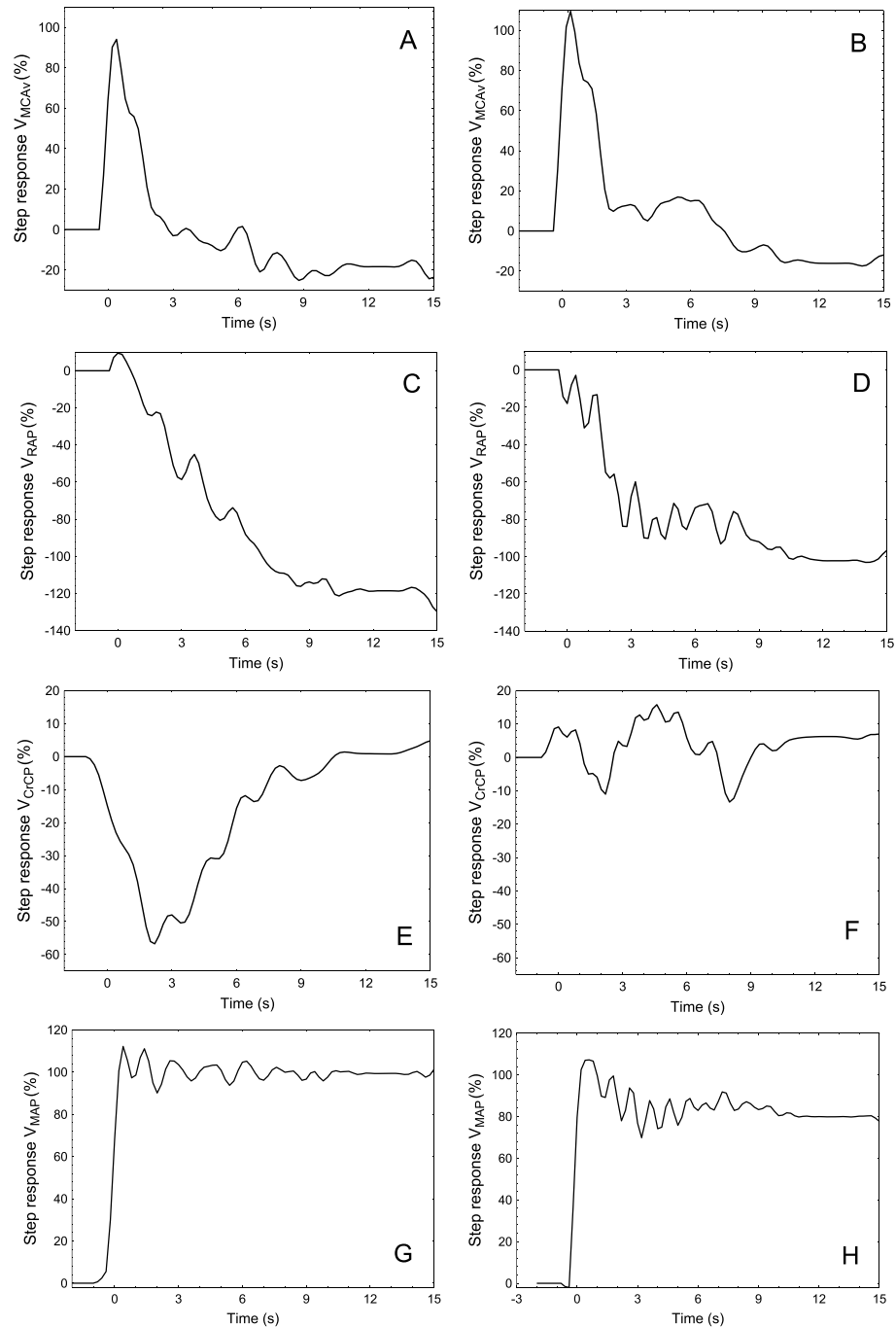


Figure 3. Step responses from representative subjects who were accepted (A), (C), (E), (G) or rejected (B), (D), (F), (H) according to statistical criteria. (A), (C), (E), (G) responses from a 61 year-old male subject with $ARI = 7.25$, $CKS_{error} = 1.8\%$. (B), (D), (F), (H) responses from a 73 year-old male subject, $ARI = 7.03$, $CKS_{error} = 18\%$. (A), (B) SRV_{MCAV} , (C), (D) SRV_{RAP} , (E), (F) SRV_{CrCP} , (G), (H) reconstructed SRV_{MAP} . Sub-plot D also illustrates the superior robustness of SRV_{RAP} , as compared to SRV_{CrCP} , against deterioration of CKS_{error} .

be extracted from its response, in comparison with more established approaches for quantification of CBF regulatory mechanisms, including CO_2 reactivity and neurovascular coupling. Of considerable importance, for the design and economy of future clinical trials, our statistical analyses did not show any effects of sex or age on SRV_{CrCP} , although this cannot be generalised to other populations, for example individuals with chronic conditions, such as arterial hypertension or diabetes mellitus.

4.2. Methodological considerations

TFA has been the main approach utilised for the assessment of dynamic CA in physiological and clinical studies. For frequency intervals where coherence meets statistical acceptance criteria (Classen *et al* 2016), estimates of gain and phase have been adopted to classify the effectiveness of dynamic CA, with phase

Table 3. Multivariate regression coefficients for significant physiological determinants of the SRV_{CrCP} response.

Co-variates →	Intercept	ARI	CrCP ₀	Heart rate	DBP
SRV_{CrCP}^{T1}	23.81 [§] (4.52)	-2.84 [#] (0.73)	-0.29 [#] (0.06)	—	—
SRV_{CrCP}^{T2}	6.76 (9.88)	-5.48 [#] (0.98)	-0.30 [#] (0.08)	0.29 [§] (0.13)	—
SRV_{CrCP}^{T3}	26.26 [§] (12.70)	-4.74 [#] (1.17)	-0.71 [#] (0.13)	—	0.40 [§] (0.18)

Values are regression slopes (SE). SRV_{CrCP}^{Tj} ($j = 1, 2, 3$): Mean step response for the critical closing pressure sub-component during time intervals $T1$ – $T3$ (see Methods); ARI: Autoregulation Index; CrCP₀: mean CrCP for the 5 min baseline recording; DBP: Mean diastolic blood pressure for the 5 min baseline recording.

[#] $p < 0.01$, [§] $p < 0.05$.

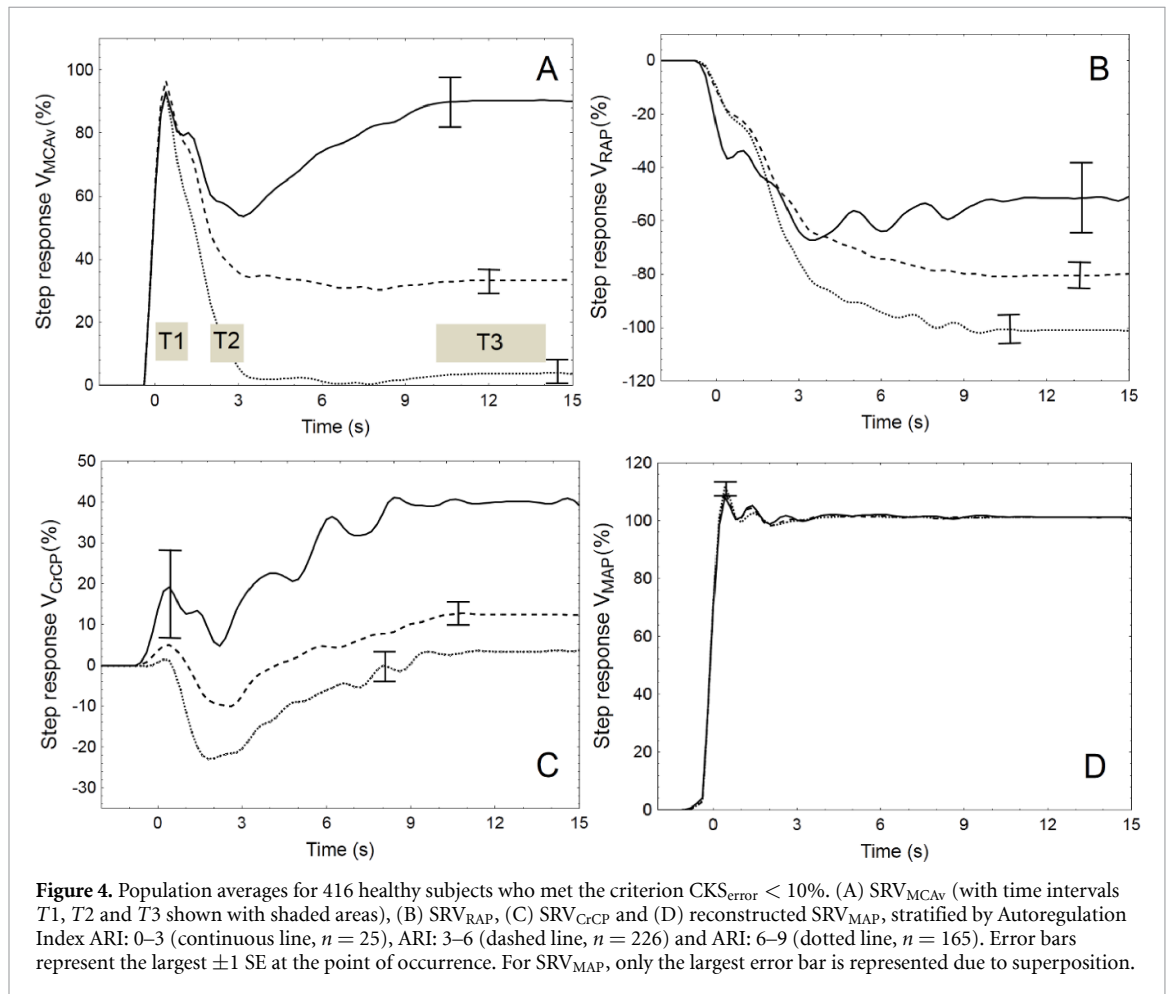


Figure 4. Population averages for 416 healthy subjects who met the criterion $CKS_{error} < 10\%$. (A) SRV_{MCAv} (with time intervals $T1$, $T2$ and $T3$ shown with shaded areas), (B) SRV_{RAP} , (C) SRV_{CrCP} and (D) reconstructed SRV_{MAP} , stratified by Autoregulation Index ARI: 0–3 (continuous line, $n = 25$), ARI: 3–6 (dashed line, $n = 226$) and ARI: 6–9 (dotted line, $n = 165$). Error bars represent the largest ± 1 SE at the point of occurrence. For SRV_{MAP} , only the largest error bar is represented due to superposition.

showing superiority in the consistency of findings in several clinical conditions (Claassen *et al* 2016, Intharakham *et al* 2019). The use of gain and phase though, is limited by the difficulty of identifying situations where these estimates are not physiologically plausible, something that is afforded by the MCAv step response (Tiecks *et al* 1995, Panerai *et al* 2016). Different from the MCAv step response though, the SRV_{CrCP} does not have a well-established temporal pattern (figure 4), or indeed, a reference model such as the 2nd order differential equation model proposed by Tiecks *et al* (1995) for the SRV_{MCAv} , that could be used as a template for quality control and the rejection of estimates that could be deemed non-physiological (Panerai *et al* 2016).

Without a well-established temporal pattern, and estimates with much larger scatter, due to the inherent limitations of deriving values of CrCP for each cardiac cycle (Panerai *et al* 2011), SRV_{CrCP} often presents outlying values that, if not discarded, could lead to distorted results. In previous studies, estimates that differed from population averages were removed after visual inspection and subjective decision-making. Although this approach led to fairly consistent results (Panerai *et al* 2020, 2021), it is clearly undesirable, mainly in clinical studies where it could lead to biased conclusions. The reliability of TFA estimates has been

underpinned by the statistical significance of the coherence function (Claassen *et al* 2016) and the variability of the input signal, in our case MAP, has also been raised as a potential determinant of reliable estimates (Elting *et al* 2020). For the case of the step responses in equation (6), the quality of the reconstructed SRV_{MAP} is also relevant, from our previous observations, and this was the reason for considering CKS_{error} as a potential determinant. Finally, the similarity of a given SRV_{CrCP} temporal pattern with other members of the ensemble, led to the formulation of the SML_{corr} parameter, aiming to mimic the process of visual inspection of temporal patterns and the subjective judgement of their similarity to other estimates.

Grubbs' statistics identifies distributions where there is at least one outlier (1950). In our case, it helped to rank the order of application of statistical criteria based on CKS_{error} , SML_{corr} , COH_{CrCP} and MAP_{power} (table 2). For SRV_{CrCP}^{T3} , after application of the second criterion (SML_{corr}), the test indicated that all outliers were removed (table 2, $p > 0.05$), which is not the case for the other two-time intervals, even after the application of all four criteria (table 2). Although the presence of some residual outliers is not desirable, there has been a clear reduction in the scatter of estimates with the application of the CKS_{error} criterion, as demonstrated by the results in figure 2 and the marked reduction in Grubbs' statistic (table 2). Further work is needed to achieve more robust estimates of SRV_{CrCP} and this might involve revisiting at the outset, current approaches for calculation of CrCP (Lopez-Magana *et al* 2009, Panerai *et al* 2011, Elizondo *et al* 2019).

Despite the large size of the population studied, the ranking of these parameters (table 2), is not immutable and future studies with different populations might show changes to that ranking. In particular, the 95% confidence limit threshold for SML_{corr} , is dependent on the sample used for its calculation (figure 1). One extreme example would be personalised care, where SML_{corr} could not be calculated, although the correlation with a reference population average could be considered as an alternative. Likewise, clinical studies with relatively small sample sizes might also lead to distortions. Therefore, there are situations where it might not be advisable to consider SML_{corr} as a statistical criterion for acceptance of SRV_{CrCP} . Although COH_{CrCP} and MAP_{power} showed a very limited contribution to improve the quality of SRV_{CrCP} estimates in the present study (table 2), it would be premature to disregard their potential contribution in future investigations involving different populations, or indeed, different approaches for the beat-to-beat estimation of CrCP.

4.3. Physiological interpretation

A sudden change in MAP leads to a corresponding simultaneous change in CBF, as reflected by the MCAv surrogate. With a working CA, flow or velocity returns to its original value, with a time-constant that is dependent on the efficiency of CA (Aaslid *et al* 1989). SRV_{MCAv} is a more general expression of this behaviour and has been reported in multiple studies, including estimates based on different modelling approaches (Panerai *et al* 2004, Chacon *et al* 2008, Panerai 2009, Ma *et al* 2016, Marmarelis *et al* 2016, Barnes *et al* 2022, Liu *et al* 2021). In the case of SRV_{RAP} , the relatively smaller number of reports in the literature show a good level of agreement, regarding its temporal pattern, possibly reflecting the myogenic pathway, leading to a gradual increase in vascular resistance as cerebral arterioles constrict to reduce CBF in response to a rise in MAP (Edwards *et al* 2001, 2004, Panerai *et al* 2006, 2011, 2012, 2020, 2021). With the increase in RAP, the corresponding subcomponent V_{RAP} , will show a negative change (equation (5)), thus indicating a reduction in CBF, or MCAv, that is also expressed by the negative excursion of SRV_{RAP} (figures 3 and 4).

The main focus of the present study though, is the understanding of the determinants of SRV_{CrCP} . Different from SRV_{MCAv} or SRV_{RAP} , the SRV_{CrCP} has not been reported by other groups. Nevertheless, the temporal patterns in figures 3 and 4 are in very good agreement with our previous reports, despite including a much larger number of subjects (Panerai *et al* 2020, 2021). In one of these studies, we have also reported the influence of dynamic CA on the temporal pattern of SRV_{CrCP} , and obtained stratified population averages that are in close agreement with the patterns in figure 4. Two differences between that study and the present one are worth mentioning. First, the sample size of the first study was 194 subjects, also extracted from the CHiASM database, and most were included in the present sample. Nevertheless, we are now including a much larger number of participants ($n = 437$) in the present study, which extends the generalisability of our findings. Second, different from the first study, we are now adopting observer-independent statistical criteria to accept/reject estimates of SRV_{CrCP} , instead of a visually based, subjective approach. From this perspective, it demonstrates that the automatic selection of SRV_{CrCP} estimates leads to very similar results to those obtained previously, with a subjective, albeit judicious, procedure.

As described above, the most immediate interpretation of the temporal patterns of SRV_{MCAv} and SRV_{RAP} is relatively straightforward, but the same cannot be said about SRV_{CrCP} . Above all, why is SRV_{CrCP} continuously rising, after 3–4 s into the response (figures 3 and 4), following the sudden decrease in RAP? And why are the final plateau levels varying with ARI? Rigorous answers to these questions will require dedicated future studies, possibly involving *in vivo* experimental work or *in vitro* isolated artery preparations. At the current stage, one speculation is that the temporal pattern of SRV_{CrCP} is expressing the endothelial

response to wall shear stress (Koller and Toth 2012). According to this mechanism, increases in CBF would lead to the initial release of nitric oxide and other mediators, thus leading to vasodilation (Paravicini *et al* 2006) before returning to baseline values as the vessel constricts. With SRV_{MCAv} remaining elevated for low values of ARI (figure 4), the correspondingly elevated values of CBF would lead to greater vasodilation, than produced by the reduced flow values observed for higher values of ARI, thus explaining the inverse relationship. In a recent study of pial artery collaterals in rats, Li and Cipolla have presented the time course of wall shear stress in response to changes in perfusion flow, with time-constants that could explain the delayed rise in SRV_{CrCP} , stimulated by the initial increase in MCAv resulting from a step change in MAP (Li and Cipolla 2022). The previous finding, that hypercapnia also leads to increases in the tail end of SRV_{CrCP} (Panerai *et al* 2020), although difficult to disentangle from the concomitant depression of dynamic CA, would reinforce the speculation that SRV_{CrCP} is reflecting metabolic-driven vasodilation.

The contribution of $CrCP_0$ to SRV_{CrCP} (table 3) reinforces the latter's association with the metabolic pathways involved in CBF regulation, as reported for the effects of hypercapnia and hypocapnia (Panerai 2003, Minhas *et al* 2018). The influence of $CrCP_0$ on SRV_{CrCP} was relatively uniform, insofar as the multiple regression coefficients had a negative sign for all three time intervals ($T1$ – $T3$, table 3), although its amplitude was twice as large for $T3$, compared with corresponding values for $T1$ and $T2$ (table 3). Therefore, a reduction in $CrCP_0$, as it would be observed during hypercapnia, would lead to an upward move of the entire SRV_{CrCP} temporal pattern, with accentuation at the tail end of the response. This behaviour confirms previous reports of the SRV_{CrCP} response to hypercapnia induced by 5% CO_2 breathing (Panerai *et al* 2020). In the present study though, it is important to note that $CrCP_0$ was not associated to $EtCO_2$ ($r = 0.045$), or to the ARI ($r = -0.040$) and hence its independent contribution to SRV_{CrCP} is a novel finding that needs to be taken into account in the interpretation of SRV_{CrCP} patterns in future clinical studies. Finally, the vasodilation corresponding to a reduction in $CrCP_0$, further reinforces our speculation that the SRV_{CrCP} temporal pattern is expressing the endothelial response to wall shear stress, which is an exciting prospect for future application of this approach in physiological and clinical investigations.

4.4. Limitations of the study

As with any studies using TCD-based approach, it is important to keep in mind that MCAv can only be regarded as a reliable surrogate of CBF if the cross-sectional area of the MCA remains approximately constant for the duration of the recordings. MCA diameter has been shown to increase with extreme values of $PaCO_2$ (Coverdale *et al* 2014, Verbree *et al* 2014), which do not apply to the conditions of our study (table 1).

We have only included beat-to-beat estimates of CrCP using the 1st harmonic method (Panerai 2003). The majority of prior studies of CrCP, independently of treating this parameter as a time-series or not, were based on the linear regression of the velocity-pressure instantaneous relationship (Early *et al* 1974, Czosnyka *et al* 1999, Dawson *et al* 1999, Weyland *et al* 2000, Aaslid *et al* 2003, Buhre *et al* 2003, Lopez-Magana *et al* 2009, Panerai *et al* 2011). In neonates, Elizondo *et al* have used an impedance based approach, to demonstrate an excellent agreement between directly observed and estimated values of CrCP (Elizondo *et al* 2019). The influence of different methods to obtain estimates of CrCP and RAP has been reported for SRV_{RAP} , but not for SRV_{CrCP} (Panerai *et al* 2011). There is a need for improvements in algorithms to extract beat-to-beat estimates of CrCP from continuous recordings of BP and MCAv, taking into consideration their potential influence on the quality of the SRV_{CrCP} . Noteworthy, our recommendations about objective statistical criteria to minimise the occurrence of outliers in SRV_{CrCP} only applies to CrCP estimates obtained with the 1st harmonic method and cannot be automatically extended to other methods that have been proposed (Czosnyka *et al* 1999, Panerai *et al* 2011, Elizondo *et al* 2019).

5. Conclusions

The temporal pattern of the CrCP response to a step change in mean arterial pressure is determined by both physiological and modelling parameters. The reconstruction error for the MAP step function is the dominant determinant of the CrCP step response quality and can be used to eliminate the large majority of outliers in SRV_{CrCP} . The efficiency of dynamic CA, expressed by the ARI metric, was confirmed as a strong determinant of the SRV_{CrCP} temporal pattern and amplitude values, and importantly, without any influences of age or sex being detected. The understanding of the determinants of SRV_{CrCP} allowed by this study, can thus provide more objective, statistically based criteria, that should lead to more robust estimation of this function in future clinical studies to be able to fully assess the value of this new approach in the diagnosis and prognosis of cerebrovascular conditions.

Data availability statement

All data that support the findings of this study are included within the article (and any supplementary information files).

Acknowledgments

A A is supported by the College of Applied Medical Sciences, University of Najran. T G R is an NIHR Senior Investigator. J S M is a Stroke Association Senior Clinical Lecturer (SCLM23_100003). L B is an NIHR funded Academic Clinical Lecturer. O L is funded by a Stroke Association Postdoctoral Fellowship (21\100029). The views expressed in this publication are those of the author(s) and not necessarily those of the NIHR, NHS or the UK Department of Health and Social Care.


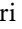


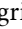

Conflict of interest

The authors declare no conflicts of interest

Ethical statement

The study was conducted in accordance with the principles embodied in the Declaration of Helsinki and in accordance with local statutory regulation. The data included in this study was amalgamated from previous studies with the following Research Ethics Committee (REC) approvals: University of Leicester Medicine & Biological Sciences (UoLMBS) REC (ref: 37467-jm591-ls:cardiovascular sciences); UoLMBS REC (ref: 31663-lb330-ls:cardiovascularsciences); Northampton REC (Ref: 11/EM/0369); Southampton and South West Hampshire REC a(Ref: 10/H0502/1); Wales REC (Ref: 15/WA/0328); Nottingham REC 1(Ref: 11/EM/0016); North East-Newcastle & North Tyneside 1 REC (Ref: 14/NE/1003)

ORCID iDs

Ronney B Panerai  <https://orcid.org/0000-0001-6983-8707>
Abdulaziz Alshehri  <https://orcid.org/0009-0006-5309-3417>
Lucy C Beishon  <https://orcid.org/0000-0002-3140-8688>
Aaron Davies  <https://orcid.org/0000-0002-5337-9371>
Victoria J Haunton  <https://orcid.org/0000-0001-6078-5469>
Emmanuel Katsogridakis  <https://orcid.org/0000-0001-8551-3910>
Man Y Lam  <https://orcid.org/0000-0002-9001-5884>
Osian Llwyd  <https://orcid.org/0000-0001-9104-3222>
Thompson G Robinson  <https://orcid.org/0000-0003-2144-2468>
Jatinder S Minhas  <https://orcid.org/0000-0002-0576-9105>

References

- Aaslid R, Blaha M, Sviri G, Douville C and Newell D W 2007 Asymmetric dynamic cerebral autoregulatory response to cyclic stimuli *Stroke* **38** 1465–9
- Aaslid R, Lash S R, Bardy G H, Gild W H and Newell D W 2003 Dynamic pressure-flow velocity relationships in the human cerebral circulation *Stroke* **34** 1645–9
- Aaslid R, Lindegaard K F, Sorteberg W and Nornes H 1989 Cerebral autoregulation dynamics in humans *Stroke* **20** 45–52
- Barnes S C, Panerai R B, Beishon L, Hanby M F, Robinson T G and Haunton V J 2022 Cerebrovascular responses to somatomotor stimulation in Parkinson's disease: a multivariate analysis *J. Cereb. Blood Flow Metab.* **42** 1547–58
- Beishon L C, Williams C A L, Robinson T G, Haunton V J and Panerai R B 2018 Neurovascular coupling response to cognitive examination in healthy controls: a multivariate analysis *Physiol. Rep.* **6** e13803
- Bendat J S and Piersol A G 1986 *Random Data Analysis and Measurement Procedures* (Wiley)
- Brasil S, de Carvalho Nogueira R, Salinet A S M, Yoshikawa M H, Teixeira M J, Paiva W S, Malbouissin L M S, Bor-Seng-Shu E and Panerai R B 2023 Critical closing pressure and cerebrovascular resistance responses to intracranial pressure variations in neurocritical patients *Neurocrit Care* **39** 399–410
- Buhre W, Heinzl F R, Grund S, Sonntag H and Weyland A 2003 Extrapolation to zero-flow pressure in cerebral arteries to estimate intracranial pressure *Br. J. Anaesth* **90** 291–5
- Burton A C 1951 On the physical equilibrium of small blood vessels *Am. J. Physiol.* **164** 319–29
- Chacon M, Nunez N, Henriquez C and Panerai R B 2008 Unconstrained parameter estimation for assessment of dynamic cerebral autoregulation *Physiol. Meas.* **29** 1179–93
- Claassen J A H R, Meel-van den Abeelen A S S, Simpson D M and Panerai R B 2016 Transfer function analysis of dynamic cerebral autoregulation: a white paper from the International Autoregulation Research Network (CARNet) *J. Cereb. Blood Flow Metab.* **36** 665–80

- Claassen J A H R, Thijssen D H J, Panerai R B and Faraci F M 2021 Regulation of cerebral blood flow in humans: physiology and clinical implications of autoregulation *Physiol. Rev.* **101** 1487–559
- Coverdale N S, Gati J S, Opalevych O, Perrotta A and Shoemaker J K 2014 Cerebral blood flow velocity underestimates cerebral blood flow during models hypercapnia and hypocapnia *J. Appl. Physiol.* **117** 1090–6
- Czosnyka M, Smielewski P, Piechnik S, Al Rawi P G, Kirkpatrick P J, Matta B F and Pickard J D 1999 Critical closing pressure in cerebrovascular circulation *J. Neurol. Neurosurg. Psychiatry* **66** 606–11
- Dawson S L, Panerai R B and Potter J F 1999 Critical closing pressure explains cerebral hemodynamics during the Valsalva maneuver *J. Appl. Physiol.* **86** 675–80
- Early C B, Dewey R C, Pieper H P and Hunt W E 1974 Dynamic pressure-flow relationships of brain blood flow in the monkey *J. Neurosurg.* **41** 590–6
- Edwards M R, Devitt D L and Hughson R L 2004 Two-breadth CO₂ test detects altered dynamic cerebrovascular autoregulation and CO₂ responsiveness with changes in arterial PCO₂ *Am. J. Physiol. Regulatory Integr. Comp. Physiol.* **287** R627–32
- Edwards M R, Lin D C and Hughson R L 2001 Modeling the interaction between perfusion pressure and CO₂ on cerebral blood flow *Adv. Exp. Med. Biol.* **499** 285–90
- Edwards M R, Shoemaker J K and Hughson R L 2002 Dynamic modulation of cerebrovascular resistance as an index of autoregulation under tilt and controlled PETCO₂ *Am. J. Physiol. Regulatory Integr. Comp. Physiol.* **283** R653–62
- Elizondo L I et al 2019 Observed and calculated cerebral critical closing pressure are highly correlated in preterm infants *Pediatr. Res.* **86** 242–6
- Elting J W et al 2020 Assessment of dynamic cerebral autoregulation in humans: is reproducibility dependent on blood pressure variability? *PLoS One* **15** e0227651
- Evans D H, Levene M I, Shortland D B and Archer L N 1988 Resistance index, blood flow velocity, and resistance area product in the cerebral arteries of very low birth weight infants during the first week of life *Ultrasound Med. Biol.* **14** 103–10
- Grubbs F E 1950 Sample criteria for testing outlying observations *Ann. Math. Stat.* **21** 27–58
- Intharakham K, Beishon L C, Panerai R B, Haunton V J and Robinson T G 2019 Assessment of cerebral autoregulation in stroke: a systematic review and meta-analysis of studies at rest *J. Cereb. Blood Flow Metab.* **39** 2105–16
- Koller A and Toth P 2012 Contribution of flow-dependent vasomotor mechanism to the autoregulation of cerebral blood flow *J. Vascular Res.* **49** 375–89
- Li Z and Cipolla M J 2022 Mechanisms of flow-mediated dilation of pial collaterals and the effect of hypertension *Hypertension* **79** 457–67
- Liu J, Guo Z N, Simpson D M, Zhang P, Liu C, Song J N, Leng X and Yang Y 2021 A data-driven approach to transfer function analysis for superior discriminative power: optimized assessment of dynamic cerebral autoregulation *IEEE J. Biomed. Health Inf.* **25** 909–21
- Lopez-Magana J, Richards H K, Radolovich D K, Kim D J, Smielewski P, Kirkpatrick P J, Pickard J D and Czosnyka M 2009 Critical closing pressure: comparison of three methods *J. Cereb. Blood Flow Metab.* **29** 987–93
- Ma H, Guo Z N, Liu J, Xing Y, Zhao R and Yang Y 2016 Temporal course of dynamic cerebral autoregulation in patients with intracerebral hemorrhage *Stroke* **47** 674–81
- Marmarelis V Z, Mitsis G D, Shin D C and Zhang R 2016 Multiple-input nonlinear modelling of cerebral haemodynamics using spontaneous arterial blood pressure, end-tidal CO₂ and heart rate measurements *Philos. Trans. R. Soc. A* **374** 20150180
- McDonald D A 1974 *Blood Flow in Arteries* (Edward Arnold)
- Minhas J S, Panerai R B and Robinson T G 2018 Modelling the cerebral haemodynamic response in the physiological range of PaCO₂ *Physiol. Meas.* **39** 065001
- Nogueira R C, Aries M, Minhas J S, Petersen N H, Xiong L, Kairnerstorfer J M and Castro P 2022 Review of studies on dynamic cerebral autoregulation in the acute phase of stroke and the relationship with clinical outcome *J. Cereb. Blood Flow Metab.* **42** 430–53
- Ogoh S, Fisher J P, Young C N and Fadel P J 2011 Impact of age on critical closing pressure of the cerebral circulation during dynamic exercise in humans *Exp. Physiol.* **96** 417–25
- Panerai R B 2003 The critical closing pressure of the cerebral circulation *Med. Eng. Phys.* **25** 621–32
- Panerai R B 2009 Transcranial Doppler for evaluation of cerebral autoregulation *Clin. Auton. Res.* **19** 197–211
- Panerai R B, Chacon M, Pereira R and Evans D H 2004 Neural network modelling of dynamic cerebral autoregulation: assessment and comparison with established methods *Med. Eng. Phys.* **26** 43–52
- Panerai R B, Eames P J and Potter J F 2006 Multiple coherence of cerebral blood flow velocity in humans *Am. J. Physiol. Heart. Circle Physiol.* **291** H251–9
- Panerai R B, Eyre M and Potter J F 2012 Multivariate modeling of cognitive-motor stimulation on neurovascular coupling: transcranial Doppler used to characterize myogenic and metabolic influences *Am. J. Physiol. Regulatory Integr. Comparative Physiol.* **303** R395–407
- Panerai R B, Haunton V J, Hanby M F, Salinet A S M and Robinson T G 2016 Statistical criteria for estimation of the cerebral autoregulation index (ARI) at rest *Physiol. Meas.* **37** 661–80
- Panerai R B, Haunton V J, Llwyd O, Minhas J S, Katsogridakis E, Salinet A S M, Maggio P and Robinson T G 2021 Cerebral critical closing pressure and resistance-area product: the influence of dynamic cerebral autoregulation, age and sex *J. Cereb. Blood Flow Metab.* **41** 2456–69
- Panerai R B, Haunton V J, Minhas J S and Robinson T G 2018 Inter-subject analysis of transfer function coherence in studies of dynamic cerebral autoregulation *Physiol. Meas.* **39** 125006
- Panerai R B, Minhas J S, Llwyd O, Salinet A S M, Katsogridakis E, Maggio P and Robinson T G 2020 The critical closing pressure contribution to dynamic cerebral autoregulation in humans: influence of PaCO₂ *J. Physiol.* **598** 5673–85
- Panerai R B, Moody M, Eames P J and Potter J F 2005 Cerebral blood flow velocity during mental activation: interpretation with different models of the passive pressure-velocity relationship *J. Appl. Physiol.* **99** 2352–62
- Panerai R B, Rennie J M, Kelsall A W R and Evans D H 1998a Frequency-domain analysis of cerebral autoregulation from spontaneous fluctuations in arterial blood pressure *Med. Biol. Eng. Comput.* **36** 315–22
- Panerai R B, Salinet A S M, Brodie F G and Robinson T G 2011 The influence of calculation method on estimates of cerebral critical closing pressure *Physiol. Meas.* **32** 467–82
- Panerai R B, White R P, Markus H S and Evans D H 1998b Grading of cerebral dynamic autoregulation from spontaneous fluctuations in arterial blood pressure *Stroke* **29** 2341–6
- Paravicini T M, Miller A A, Drummond G R and Sobey C G 2006 Flow-induced cerebral vasodilatation in vivo involves activation of phosphatidylinositol-3 kinase, NADPH-oxidase, and nitric oxide synthase *J. Cereb. Blood Flow Metab.* **26** 836–45

- Puppo C, Camacho J, Varsos G V, Yelicich B, Gomez H, Moraes L, Biestro A and Czunosnyka M 2016 Cerebral critical closing pressure: is the multiparameter model better suited to estimate physiology of cerebral hemodynamics? *Neurocrit Care* **25** 446–54
- Soehle M, Czunosnyka M, Pickard J D and Kirkpatrick P J 2004 Critical closing pressure in subarachnoid hemorrhage: effect of cerebral vasospasm and limitations of a transcranial Doppler-derived estimation *Stroke* **35** 1393–8
- Tiecks F P, Lam A M, Aaslid R and Newell D W 1995 Comparison of static and dynamic cerebral autoregulation measurements *Stroke* **26** 1014–9
- van Veen T, Panerai R B, Haeri S, Zeeman G G and Belfort M A 2015 Effect of breath-holding on cerebrovascular hemodynamics in normal pregnancy and preeclampsia *J. Appl. Physiol.* **118** 858–62
- Verbree J, Bronzwaer A S G T, Ghariq E, Versluis M J, Daemen M J A P, van Buchem M A, Dahan A, van Lieshout J J and van Osch M J P 2014 Assessment of middle cerebral artery diameter during hypocapnia and hypercapnia in humans using ultra-high-field MRI *J. Appl. Physiol.* **117** 1084–9
- Welch P D 1967 The use of the fast Fourier transform for the estimation of power spectra: a method based on time averaging over short, modified periodograms *IEEE Trans. Audio Electroacoust.* **15** 70–73
- Weyland A, Buhre W, Grund S, Ludwig H, Kazmaier S, Weyland W and Sonntag H 2000 Cerebrovascular tone rather than intracranial pressure determines the effective downstream pressure of the cerebral circulation in the absence of intracranial hypertension *J. Neurosurg. Anesth.* **12** 210–6